APS physics

CHORUS

This is the accepted manuscript made available via CHORUS. The article has been published as:

Time-dependent broken-symmetry density functional theory simulation of the optical response of entangled paramagnetic defects: Color centers in lithium fluoride

Benjamin G. Janesko

Phys. Rev. B **97**, 085138 — Published 21 February 2018

DOI: 10.1103/PhysRevB.97.085138

Time-dependent symmetry-broken density functional theory simulation of the optical response of entangled paramagnetic defects: Color centers in lithium fluoride

Benjamin G. Janesko*

Department of Chemistry & Biochemistry, Texas Christian University,

2800 S. University Dr., Fort Worth, TX 76129, USA

Abstract

Parameter-free atomistic simulations of entangled solid-state paramagnetic defects may aid rational design of devices for quantum information science. This work applies time-dependent density functional theory (TDDFT) embedded-cluster simulations to a prototype entangled-defect system, two adjacent singlet-coupled F color centers in lithium fluoride. TDDFT calculations accurately reproduce the experimental visible absorption of both, isolated and coupled F centers. The most accurate results are obtained by combining spin symmetry breaking to simulate strong correlation, a large fraction of exact (HF) exchange to minimize the trapped electrons' self-interaction error, and a standard semilocal approximation for dynamical correlations between the defect electrons and the surrounding ionic lattice. These results motivate application of two-reference correlated *ab initio* approximations to the M-center, and application of TDDFT in parameter-free simulations of more complex entangled paramagnetic defect architectures.

I. INTRODUCTION

Optically addressable paramagnetic defects in wide-bandgap semiconductors and insulators show enormous promise for quantum information science.[1] Such defects have been used as qubits for quantum computing,[2–4] fluorescent probes[5] and sensors,[6] narrowband single-photon emitters,[7] and nanoscale magnetometers.[8,9] Atomistic *ab initio* simulations of such defects' structure,[10] optical response,[11,12] and quantum-mechanical entanglement are critical for interpreting experiments. Such simulations could ultimately aid rational design of practical devices.[13,14] This fact motivates development and testing of accurate, minimally empirical, and computationally efficient approaches for atomistic simulation of such defects.

A simple model system of optically addressable paramagnetic defects is alkali halide F-centers (color centers), in which a single electron is trapped at an anion vacancy.[15–17] The trapped electron forms a "quasi-atom" analogous to hydrogen atom.[18] Atomistic simulations have confirmed the anion-vacancy model of the F-center,[19] characterized the detailed structure of its electron density,[20] and provided accurate treatments of its geometry[21] and optical spectra.[22,23] An important recent study demonstrated that both, embedded-cluster *ab initio* quantum chemistry, and periodic supercell many-body perturbation theory (GW+BSE),[23] provide quantitative agreement with the experimental absorption spectra of isolated F-centers.[24] Follow-up studies give insight into the Mollwo-Ivey relation between lattice parameter and absorption energy.[25]

I recently showed[26] that the lithium fluoride M-center defect, a "quasi-H_2 molecule" with two singlet-coupled electrons trapped at adjacent anion vacancies,[27,28] provides a simple and experimentally realized model system for entanglement among optically addressable paramagnetic defects. The M-center is analogous to the singlet ground state of H_2 with a stretched H-H bond, a "textbook" system for strong correlation and entanglement.[29–36] This system's singlet ground state at the limit of long bound length is the maximally entangled two-qubit state $|\Psi^+\rangle = \frac{1}{\sqrt{2}}\left(|\uparrow\downarrow\rangle + |\downarrow\uparrow\rangle\right)$ invoked in quantum information science.[37] Simple molecular-orbital/band-structure pictures (single-reference symmetry-restricted Hartree-Fock calculations) qualitatively fail to reproduce the M-center's experimental ground-state magnetization and absorbance spectrum,[38,39] just as they qualitatively fail to reproduce the excitation energies of stretched H_2.[40] However, Ref.[26] showed that a broken-spin-symmetry time-dependent Hartree-Fock treatment of the first singlet excitation energy, "dressed" with

approximate corrections for electron correlation,[24] predicted an M-center absorbance peak within ~ 0.3 eV of experiment.[26] Improved *ab initio* results would in principle require correlated multireference calculations, whose computational expense makes them impractical for large-scale simulations of realistic device architectures.

Kohn-Sham density functional theory (DFT) has been widely applied as a solution to such difficulties. DFT simulations, using relatively simple density functional approximations (DFAs) for the exact exchange-correlation functional, combine mean-field cost with useful accuracy for many systems.[41–43] Hybrid DFAs incorporating a fraction of exactly computed (Hartree-Fock-like, HF) exchange are particularly popular, as they tune the "zero-sum" tradeoff between electron self-interaction and simulation of electron correlation in covalent bonds.[32] Broken-spin-symmetry Kohn-Sham calculations using wavefunctions that are not eigenfunctions of $\hat{S}^2$ (*i.e.*, that are not pure singlet, doublet, triplet, etc. states), can sometimes treat properties that would otherwise require multireference *ab initio* theory.[44] Ref.[26] reviews the classic example of the singlet ground-state energy of stretched H_2. This is above the triplet energy in symmetry-restricted calculations with standard DFAs and Hartree-Fock theory, but qualitatively correct in broken-symmetry calculations placing spin-up and spin-down electrons on different atoms. An enormous range of spin-projection and effectively multireference methods have been proposed to connect broken-symmetry DFT calculations back to states of the desired symmetry.[45–50] (Specialists may note the argument that the exact ground-state wavefunction of the noninteracting Kohn-Sham reference system need not be an eigenfunction of $\hat{S}^2$, or of any other two-electron operator.[51]) Practical applications of broken-symmetry DFT are exemplified in recent treatments of magnetic couplings.[52]

DFT is also applied beyond the ground state.[53] Adiabatic linear response time-dependent density functional theory (TDDFT) calculations, performed using standard ground-state DFAs, can accurately simulate the character and vertical excitation energy of many singly-excited states.[54–57] Refs.[58,59] review connections between TDDFT and the many-body Green's function approaches applied in Ref.[24]. The combination of TDDFT and spin symmetry breaking is particularly powerful for multireference systems. TDDFT excitations computed from broken-symmetry singlet ground states have been recently applied to long-range charge-transfer excitations[60] and electronic spectra of open-shell singlet diradical nickel complexes.[61] CI-singles (Tamm-Dancoff) Hartree-Fock calculations from broken-symmetry ground states provide qualitatively reasonable singlet excitation energies for dissociating H_2,

though they can be problematic for triplet states.[62] TDDFT from symmetry-unrestricted paramagnetic states has also been applied to optical absorption spectra of oxo and peroxo dicopper(II) complexes,[63] dynamic polarizability of open-shell molecular systems,[64] and electronic circular dichroism spectra of open-shell Cr(III) compounds.[65] Other relevant work includes spin-flip TDDFT treatments of ground states,[66,67] the linear response of projected Hartree-Fock theory[50,68] and noncollinear spin density functional theory,[69] and the use of symmetry-broken wavefunctions as reference in semiempirical CI-singles.[70]

This work reports the performance of broken-symmetry embedded-cluster TDDFT calculations, using various approximate DFAs, in simulating the electronic structure and absorbance spectra of isolated paramagnetic F-centers and strongly correlated adjacent singlet-coupled F-centers. While Hartree-Fock theory itself tends to overestimate the excitation energies, DFAs incorporating large fractions of HF exchange provide balanced treatments of both F- and M- centers. The minimally empirical long-range-corrected DFA LC-ωPBE, and a screened hybrid DFA combining 100% screened HF exchange with long-range PBE exchange, provide balanced performance for both systems. This motivates applying broken-symmetry TDDFT to simulate more complicated coupled-defect architectures relevant to quantum information science.

II. COMPUTATIONAL METHODS

This work uses the development version of the Gaussian suite of programs[71] to perform generalized Kohn-Sham calculations with nonlocal, nonmultiplicative exchange-correlation potentials for DFAs incorporating HF exchange.[72,73] Computational details closely follow the embedded-cluster calculations of Ref.[26], with a more sophisticated extrapolation to the basis set and cluster embedding limits. Atomic positions are taken from defect-free lattices at the experimental LiF lattice constants 2.02 Angstrom.[74] The single F-center is treated as a $Li_{14}F_{12}^{+}$ cluster treated completely quantum-mechanically (QM).[38] This cluster is surrounded by a $Li_{150}F_{128}$ cluster of embedding potentials, then by a $Li_{2026}F_{2048}$ cluster of isolated point charges ± 1 (cluster "F1"). The M-center lying along the $\langle 110 \rangle$ direction is treated as a $Li_{10}F_{18}^{-10}$ QM cluster, embedded in a surrounding $Li_{136}F_{150}$ cluster of embedding potentials, surrounded by a $Li_{3730}F_{3704}$ cluster of isolated point charges (cluster "M1"). As in Ref.[26], calculations treat the Li^{+} embedding potential as a point charge $+1$ surrounded by the

SBKJC effective core potential (ECP),[75] and treat the F^- embedding potential as a point charge -1 surrounded by the SBKJC ECP of Na^+. While the assumption that 10-electron ions F^- and Na^+ have identical cores is clearly imperfect, Ref.[26] showed that calculations with this assumption largely reproduce previous work, suggesting that the detailed form of the embedding potential is not critical for the effects of interest here. Unless noted otherwise, calculations use the cc-pVDZ basis set on the QM region, and include "dummy" hydrogen atom basis sets at the defect centers.

The embedded-cluster calculations F1 are extrapolated as follows. The time-dependent unrestricted Hartree-Fock/cc-pVDZ first excitation energy of cluster F1 is 6.2255 eV, vs. 6.1672 eV for much larger embeddings up to $Li_{1672}F_{1732}$ embedding potentials and $Li_{504}F_{444}$ point charges, giving a 0.06 eV redshift for the embedding potential. Calculations with larger QM regions give first excitation energies 6.1672 eV $Li_{14}F_{12}$, 6.1043 eV $Li_{14}F_{18}$, 6.0680 eV $Li_{38}F_{18}$, 6.0489 eV $Li_{38}F_{54}$. Extrapolation as N^{-1}, where N is the number of atoms in the QM region, suggests a QM-cluster limit excitation energy 6.02 eV and a 0.15 eV redshift to extrapolate the QM region. Calculations on the F1 cluster give excitation energies 6.0738 eV in the cc-pVTZ basis set and 6.0488 eV in the cc-pVQZ basis set. Extrapolation as Z^{-3} where Z is the basis set cardinality suggests a basis set limit value 6.03 eV and a 0.13 eV redshift for basis set corrections to the F1/cc-pVDZ results. Combined, these suggest a 0.06+0.15+0.13=0.34 eV total redshift to F1/cc-pVDZ results to reach the basis-set and cluster size limit. This shift is smaller than the (5.99-5.50)=0.45 eV redshift between $Li_{14}F_{12}$/cc-pVDZ and $Li_{62}F_{62}$ complete basis set CASPT2(ROHF) results reported in Ref.[24], consistent with the larger basis set demands of the latter's correlated *ab initio* calculations. Additional redshifts of 0.21 eV for ground- and excited-state geometry relaxation and 0.09 eV for electron-phonon coupling are taken from Ref.[24].

The embedded-cluster calculations M1 are extrapolated as follows. The broken-symmetry time-dependent unrestricted Hartree-Fock/cc-pVDZ first excitation energy of cluster M1 is 4.1835 eV, vs. 4.1834 eV for much larger embeddings up to $Li_{136}F_{150}$ embedding potentials and $Li_{6934}F_{6908}$ point charges, giving negligible redshifts for embedding potential. Calculations with larger QM regions give first excitation energies 4.1835 eV $Li_{10}F_{18}$, 4.1478 eV $Li_{22}F_{18}$, 4.1285 eV $Li_{22}F_{26}$. Extrapolation as N^{-1} suggests a QM-cluster limit excitation energy 4.05 eV and a 0.13 eV redshift to extrapolate the QM region. Broken-symmetry TDUHF calculations on the M1 cluster give excitation energies 4.1459 eV in the cc-pVTZ

basis and 4.1273 eV in the cc-pVQZ basis, such that extrapolation as Z^{-3} gives a basis set limit 4.12 eV and a 0.06 eV redshift for basis set corrections to M1/cc-pVDZ results. These basis set effects for the M center $^1\Sigma_g^+ \rightarrow {}^1\Sigma_u^+$ excitation are smaller than the basis set effects on the F center 1s→2p excitation, as expected. Combined, these suggest an 0.13+0.06=0.18 eV total redshift to M1/cc-pVDZ results to reach the basis-set and cluster size limit. Additional redshifts of 0.21 eV for ground- and excited-state geometry relaxation and 0.09 eV for electron-phonon coupling are assumed to be identical to those of the F-center.

A major part of this work involves comparing the performance of different DFAs. Calculations compare a broad range of "standard" DFAs implemented in the Gaussian package.[71] The simplest tested approximations are the local spin-density approximation LSDA[76] and the Xα method combining rescaled LSDA exchange and no correlation functional.[77] Tested generalized gradient approximations (GGAs) include the nonempirical Perdew-Burke-Ernzerhof (PBE) and Perdew-Wang PW91 GGAs[78,79] and the empirical B97-1,[80] B97-2,[81] B97-D,[82] HCTH93,[83] HCTH147,[84] and HCTH407,[85] GGAs. (While empirical dispersion corrections as in B97-D are not expected to significantly affect the present results, their importance in other areas[86] motivates inclusion here.) Tested meta-GGAs include the nonempirical Tao-Perdew-Staroverov-Scuseria TPSS[87] and empirical M06-L.[88] Tested global hybrids including a constant fraction of HF exchange include the arguably nonempirical[89] PBE0 (25% HF exchange),[90,91] and the empirical O3LYP (11.6%),[92] B3LYP (20%),[79,93–96] BHHLYP (50%),[79,93,94] and M06-HF (100%)[97] global hybrids. Calculations also test the combination of 100% HF exchange with the LDA or PBE correlation functional, denoted "HFLDA" or "HFPBE", and the APFD combination of 41.1% B3PW91 and 58.9% PBE0 plus dispersion corrections.[98] Tested range-separated hybrids include the HSE06[99,100] and HISS[101] screened hybrids incorporating no long-range HF exchange, as well as a "HSE100" combining 100% short-range HF exchange with no long-range HF exchange. Tested long-range-corrected hybrids, whose inclusion of additional long-range HF exchange is known to improve many excited states,[102] include LC-ωPBE,[103] ωB97X-D,[104] and CAM-B3LYP.[105]

Other computational details are as follows. TDDFT calculations are performed with vs. without the Tamm-Dancoff approximation. Calculations on the M-center are performed from both symmetric and broken-spin-symmetry singlet states. The broken-spin absorption is assumed to correspond to the first excited state with a non-negligible computed transition dipole moment. All corrections are assumed to be transferable between the tested

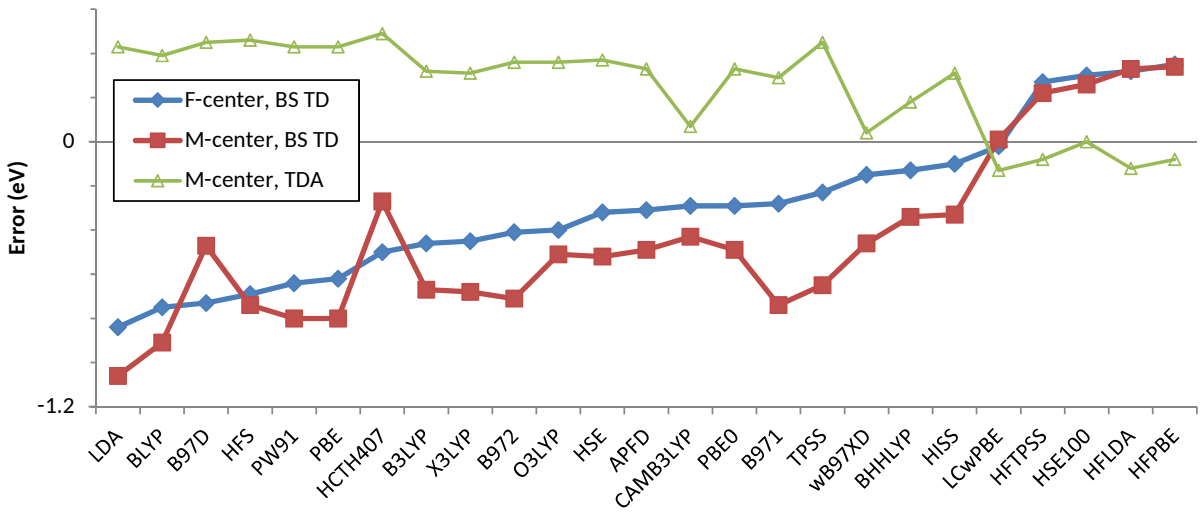

FIG. 1. Signed error (theory-experiment, eV) in the excitation energies of F- and M-centers predicted by time-dependent DFT using various DFAs. Results are shown for broken-symmetry TD calculations on an isolated F-center, and broken-symmetry TD and symmetry-restricted TDA calculations on an M-center.

DFT methods, and between TD, TDA, and band structure calculations. All excitations are confirmed be dipole-allowed states with significant nonzero predicted transition dipole moments. Atom-averaged quantities are obtained using Mulliken population analysis.

III. RESULTS

A. Isolated paramagnentic defect

Figure 2 presents a single F-center's three-dimensional structure and ground-state spin density , as well as total and spin densities inside the defect computed with representative DFAs. The unpaired electron density is localized inside the defect, yielding a non-nuclear attractor[20] in the total density.

Table I includes additional detail on different DFAs' predictions for the F-center defect electronic structure. The table includes the total electron density at the non-nuclear attractor ρ_{NNA}, and the total Mulliken charge & spin density Li_Q and Li_M of the lithium atoms ajacent to the defect. DFAs that localize the trapped electron inside the defect tend to give

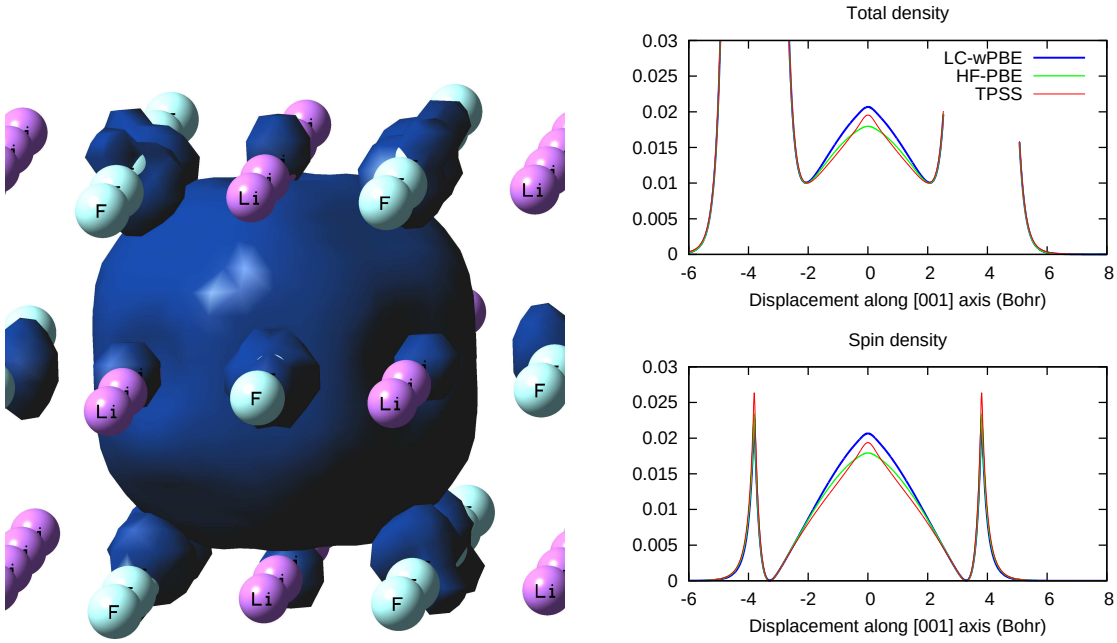

FIG. 2. Structure and spin density of an isolated F-center defect. (Left) Three-dimensional structure and LC-ωPBE spin density, isosurface 0.0004 bohr^{-3}. (Right) Defect total and spin densities along along the [100] axis, evaluated for representative DFAs.

Li_Q approaching +1, and Li_M approaching 0.

Table I also presents the predicted symmetry-unrestricted TD and TDA first excitation energies of a single F-center. Band structure excitation energies (HOMO-LUMO gaps), and TD first excitation energies of isolated H atom, are reported for comparison. Figure 1 summarizes the errors relative to experiment. Results are sorted from lowest to highest F-center TD excitation energy. These spin-unrestricted doublet calculations have little spin contamination, with ground- and excited-state $\left\langle \hat{S}^2 \right\rangle$ between 0.750 and 0.754. All of the tested DFAs predict that the F-center excitation is a 1s$\rightarrow$2p -like excitation of the trapped electron "quasi-atom".

The trends for single trapped electrons in Table I and Figure 1 are consistent with the previous literature on time-dependent DFT. The best agreement with experiment comes from DFAs that combine a semilocal correlation functional with a large fraction of HF exchange, particularly the long-range-corrected LC-ωPBE. TD and TDA results are nearly identical, consistent with previous studies of the Tamm-Dancoff approximation.[106] Band energies do not reproduce the experimental absorption energy, consistent with their lack of

particle-hole interactions.[24,107] Similar results are found for the M-center (not shown).

The trends among different DFAs are also broadly consistent with the literature. Time-dependent Hartree-Fock calculations (entry "HF") give an absorption energy $\sim$ 0.5 eV above experiment. This is consistent with the important role of dynamical correlation seen in Refs.[21,24]. (The TDHF F-center calculations in Ref.[26], unlike the present calculations, included an approximate correction for dynamical correlation extrapolated from the *ab initio* calculations in Ref.[24].) Adding semilocal correlation corrections to Hartree-Fock theory (entries "HFLDA" and "HFPBE") modestly improves the predicted F-center excitation energies. In contrast to these full-range HF results, DFAs that do not include any HF exchange underestimate the excitation energy. This is consistent with these DFAs' known self-interaction error[108] and their resulting tendency to underestimate valence and Rydberg excitations.[57] However, it is important to note that long-range HF exchange is not required to accurately predict the F-center excitation energy. This conclusion is particularly encouraging for periodic supercell simulations of paramagnetic defects, as long-range HF exchange can be computationally expensive in such simulations.[109] The "middle-range" HISS hybrid gives an excitation energy close to LC-ωPBE. The HSE100 hybrid of 100% screened HF exchange approaches HFPBE (100% full-range HF exchange). This is again consistent with the literature on range separation in DFAs, particularly Ref.[110]. That reference demonstrated that many properties of interest, particularly in condensed phases, depend on the "middle-range exchange" between electrons separated by $\sim 1-2$ bohr (or equivalently 1-2 chemical bond lengths). For many properties, including low-lying Rydberg state excitations, polarizabilities of H_2 chains, and Raman activities, screened hybrid DFAs incorporating no asymptotic long-range HF exchange can provide performance comparable to long-range-corrected hybrids incorporating 100% asymptotic long-range HF exchange. (However, truly "long-range" properties such as long-range beween-molecule chage transfer do still require long-range HF exchange.[111])

Ref.[26] illustrated the utility of comparing the F-center "quasi-atom" to hydrogen atom itself. Accordingly, Table I also reports the first bright state excitation predicted for H atom. Trends in the different DFAs' predictions for the F-center excitation energy generally mirror trends for hydrogen atom. This is consistent with the "quasi-atom" model of the F-center as a single electron confined by the surrounding ionic lattice.[18]

Additional insight into the trends in Table I comes from the trends in electron density

TABLE I. Excitation energies (eV) of a single isolated F-center, predicted using a variety of density functional approximations. Results are shown for time-dependent density functional theory TDDFT, the Tamm-Dancoff approximation TDA, and band energies "band". Isolated hydrogen atom $1s \rightarrow 2P$ TD excitation energy "Hatom", total density at the non-nuclear attractor ρ_{NNA} (au), and atom-averaged partial charge Li_Q and spin Li_M for the Li atoms closest to the defect are included . DFAs are sorted from smallest to largest predicted TDDFT excitation energy.

Method	TDDFT	TDA	Band	Hatom	ρ_{NNA}	Li_Q	Li_M
Experiment	5.08						
LDA	4.24	4.3	3.85	9.87	1.57	0.558	0.160
BLYP	4.33	4.38	4.14	10.18	1.809	0.625	0.123
B97D	4.35	4.43	4.19	10.53	1.462	0.69	0.109
HFS	4.39	4.45	4.02	9.71	1.626	0.536	0.154
PW91	4.44	4.49	4.17	10.34	1.641	0.63	0.13
PBE	4.46	4.51	4.17	10.24	2.069	0.632	0.13
HCTH407	4.58	4.67	4.28	10.46	2.069	0.665	0.143
B3LYP	4.62	4.67	5.69	10.4	1.829	0.661	0.118
X3LYP	4.63	4.68	5.8	10.42	1.828	0.657	0.118
B972	4.67	4.72	5.75	10.64	1.614	0.715	0.112
O3LYP	4.68	4.73	5.23	10.46	1.718	0.689	0.121
HSE	4.76	4.81	5.3	10.5	1.655	0.679	0.118
APFD	4.77	4.78	5.97	10.49	1.677	0.685	0.12
CAMB3LYP	4.79	4.84	8.39	10.4	1.818	0.639	0.122
PBE0	4.79	4.84	6.11	10.51	1.663	0.683	0.12
B971	4.8	4.86	5.74	10.56	1.993	0.68	0.129
TPSS	4.85	4.92	4.78	10.48	1.955	0.68	0.114
wB97XD	4.93	5.02	9.53	10.39	1.944	0.69	0.135
BHHLYP	4.95	5	8.02	10.71	1.883	0.714	0.104
HISS	4.98	5.03	5.82	10.74	1.72	0.677	0.109
LCwPBE	5.06	5.12	10.86	10.53	2.069	0.636	0.119
HFTPSS	5.35	5.43	11.8	11.18	1.6	0.827	0.089
HSE100	5.38	5.43	8.91	11.31	1.823	0.831	0.086
HFLDA	5.4	5.45	12.23	11.45	2.017	0.843	0.081
HFPBE	5.43	5.49	12.05	11.32	1.797	0.829	0.089
HF	5.53	5.59	12.45	11.24	2.069	0.828	0.071

in Table I. DFAs that localize the trapped electron inside the vacancy, and give Li_Q near 1 and Li_M near 0, also tend to give relatively large excitation energies, as expected from their enhanced localization. In contrast, the computed total density at the NNA proves to have a weaker correlation with the predicted excitation energies.

B. Adjacent singlet-coupled defects

Figure 3 presents two singlet-coupled F centers' three-dimensional structure and ground-state spin density, evaluated with symmetry-broken DFT. The effect of symmetry breaking

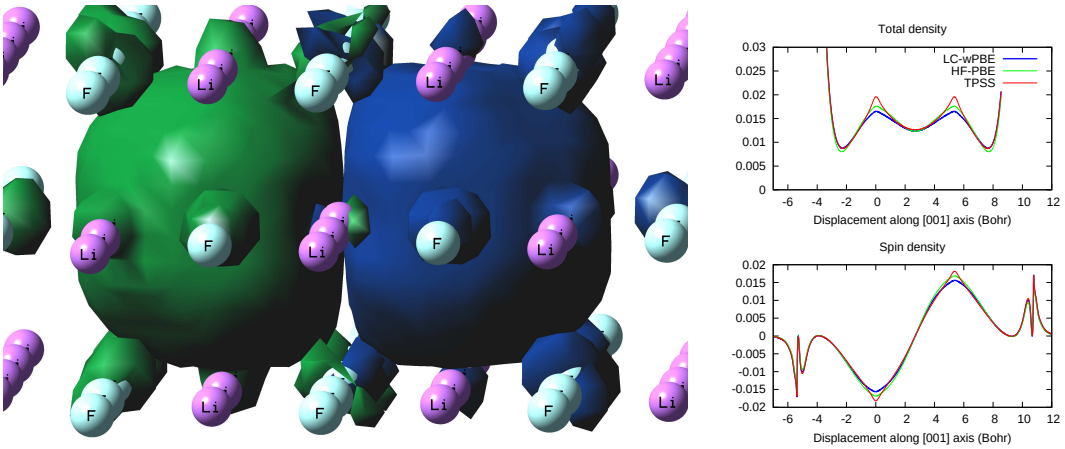

FIG. 3. Structure and spin density of two coupled F-center defects. (Left) Three-dimensional structure and LC-ωPBE spin density, isosurface 0.0004 bohr^{-3}. Blue and green denote different spin polarizations. (Right) Defect total and spin densities along along the [110] axis, evaluated for representative DFAs.

is clear: one defect site contains mostly α-spin electrons, the other contains mostly β-spin electrons. Table II presents the computed Mulliken charge and spin density Li_Q and Li_M of the four Li atoms closest to the left F-center. The variations among different DFAs are somewhat larger than for the isolated F-center (Table I). Increasing the fraction of HF exchange increases the spin polarization, increasing both the charge and spin on the atoms.

Table III presents the predicted symmetry-restricted and symmetry-broken TD and TDA first excitation energies of the two adjacent singlet-coupled defects in the M-center. Figure 1 summarizes the signed errors in F-center TD, M-center symmetry-restricted TDA, and M-center spin-symmetry-broken (BS) TD approximations. In symmetry-restricted calculations, all tested DFAs give singlet→triplet excitations with negative excitation energies, consistent with previous evidence that the M-center has a singlet-triplet instability comparable to H_2 stretched beyond the Coulson-Fischer point.[26,38]

The symmetry-restricted TD and TDA excitation energies depend only modestly on the choice of DFA. DFAs with large fractions of HF exchange tend to predict TD and TDA excitation energies below those of DFAs without HF exchange. This trend is consistent with the results seen in Table III for stretched H_2. The TDA first singlet excitation energies are higher and somewhat more accurate than TD. The rather good performance of symmetry-restricted TDA for the M-center excited state is comparable to that seen previously for

TABLE II. Atom-averaged partial charge Li_Q and spin Li_M for the Li atoms closest to the left defect, in two adjacent singlet-coupled F-center defects. DFAs are sorted from smallest to largest predicted Li_Q.

Method	Li_Q	Li_M
HFS	-0.096	0.250
LDA	-0.065	0.199
BLYP	0.011	0.189
PW91	0.024	0.204
PBE	0.026	0.205
LCwPBE	0.072	0.212
CAMB3LYP	0.073	0.210
TPSS	0.078	0.194
X3LYP	0.087	0.199
B3LYP	0.090	0.199
B97D	0.103	0.178
SLC-PBE	0.107	0.211
B971	0.112	0.184
HSE	0.114	0.204
HCTH407	0.115	0.231
wB97XD	0.117	0.209
APFD	0.124	0.207
HISS	0.126	0.200
PBE0	0.126	0.206
O3LYP	0.147	0.208
B972	0.151	0.173
BHHLYP	0.188	0.195
MN15L	0.225	0.157
HF	0.368	0.172
HFTPSS	0.372	0.188
HSE100	0.374	0.186
HFPBE	0.376	0.190
HFLDA	0.395	0.179

symmetry-restricted CI-singles calculations on H_2.[62] Overall, symmetry-restricted TDA excitations, computed using DFAs combining semilocal correlation with large large fractions of HF exchange, tend to be rather accurate for the M-center.

In contrast to the case of unstable symmetry-restricted reference wavefunctions, the stable symmetry-broken excitation energies depend rather strongly on the choice of DFA. As for the F-center, TD and TDA results obtained with a given DFA are nearly identical.[106] Trends in different DFAs mirror those seen for the isolated F-center, as well as for isolated H atom and symmetry-broken H_2. In all of these cases, DFAs without HF exchange underestimate the excitation energy, while those with 100% HF exchange overestimate it.

Dynamical correlation proves to have a particularly large effect in broken-symmetry simulations of the M-center. Broken-symmetry TDHF strongly overestimates the M-center

TABLE III. Excitation energies (eV) of a single M-center, predicted with a variety of density functionals and symmetry-restricted and symmetry-broken TD and TDA calculations. TD results for H_2, with bond length 2.85 Angstrom equal to the M-center's defect-defect separation are included for comparison.

	Symmetric			Symmetry broken		
Method	TD	TDA	H_2	TD	TDA	H_2
Experiment	2.79					
LDA	1.84	3.25	3.48	1.76	2.25	4.03
BLYP	1.91	3.21	3.42	1.91	2.09	4.64
B97D	1.96	3.26	3.44	2.35	2.64	8.05
Xα	1.83	3.28	3.48	2.09	2.19	6.27
PW91	1.90	3.24	3.45	2.02	2.16	6.41
PBE	1.89	3.25	3.46	2.02	2.16	6.27
HCTH147	1.95	3.28	3.43	2.34	2.62	7.11
HCTH93	1.95	3.24	3.42	2.33	2.52	6.88
HCTH407	1.94	3.33	3.42	2.57	2.70	7.51
B3LYP	1.93	3.13	3.40	2.14	2.26	5.46
X3LYP	1.93	3.13	3.39	2.14	2.26	5.57
B972	1.95	3.18	3.41	2.10	2.41	8.63
O3LYP	1.94	3.18	3.39	2.29	2.37	4.90
HSE	1.93	3.19	3.41	2.31	2.41	7.16
APFD	1.93	3.15	3.42	2.32	2.42	6.87
CAM-B3LYP	1.87	2.89	3.37	2.38	2.47	5.96
PBE0	1.93	3.15	3.41	2.33	2.43	7.13
B971	1.94	3.09	3.41	2.06	2.41	8.22
TPSS	1.94	3.26	3.53	2.15	2.24	3.20
ωB97X-D	1.88	2.84	3.40	2.33	4.70	7.63
BHHLYP	1.95	3.00	3.32	2.47	2.55	6.57
HISS	1.94	3.12	3.35	2.49	2.88	7.94
LC-ωPBE	1.80	2.69	3.36	2.82	2.88	7.77
HFTPSS	1.88	2.74	2.96	3.02	3.09	8.67
HSE100	1.95	2.81	3.19	3.05	3.12	9.40
HFLDA	1.94	2.68	3.14	3.11	3.18	7.60
HFPBE	1.92	2.74	3.18	3.13	3.19	9.29
HF	1.95	2.75	3.17	3.69	3.77	9.38

excitation energy, while the HFLDA, HFPBE, HFTPSS combinations of HF exchange with a DFA for dynamical correlation are significantly more accurate. (The TDHF M-center calculations in Ref.[26], unlike the present calculations, included an approximate correction for dynamical correlation taken from Ref.[24].) This appears to result from an improved treatment of the trapped electrons' interactions with the defect walls. Broken-symmetry TD calculations on isolated H_2 molecule shows a much smaller effect of the dynamical correlation functional: HF and HFPBE excitation energies differ by < 0.1 eV for H_2, > 0.5 eV for the M-center.

IV. DISCUSSION

The results presented here show that time-dependent DFT can provide accurate treatments of the optical response of both isolated and coupled paramagnetic defects in lithium fluoride. Density functional approximations that combine a large fraction of HF exchange, with a standard semilocal approximation for dynamical correlation, prove to give a balanced treatment of both the defect electron and its coupling with the surrounding ionic lattice. Careful extrapolation to the basis-set and cluster size limits gives confidence in these embedded-cluster results.

Overall, the LC-ωPBE long-range-corrected DFA gives the best agreement with experiment, giving F-center, symmetry-restricted TDA M-center, and broken-symmetry TD M-center excitations all within 0.03 eV of the experimental values. This is consistent with LC-ωPBE known accuracy for valence, Rydberg, and charge-transfer excited states.[103] The "HSE100" combination of 100% screened HF exchange and semilocal correlation gives results nearly comparable to the full-range HF exchange HFPBE. This shows that long-range HF exchange is not necessary for simulating these localized trapped-electron defects, consistent with previous comaprisons of screened vs. long-range-corrected DFAs for some other properties improved by long-range correction.[110]

The success of symmetry-broken DFT is consistent with the physical picture of the M-center defect as two strongly correlated trapped electrons, weakly correlated with the surrounding lattice. Symmetry-broken HF-PBE is from this perspective a symmetry-broken approximation to a two-component open-shell reference, combined with a simple DFT treatment of the trapped electrons' correlations with the surrounding crystal lattice. This further suggests that a relatively simple two-configuration wavefunction, combined with second-order many-body corrections, could provide accurate *ab initio* predictions for M-center excitations.

Overall, these results provide a framework for future atomistic simulations of coupled, optically addressable paramagnetic defects in quantum information science.

This work was supported by the National Science Foundation DMR-1505343.

V. REFERENCES

* b.janesko@tcu.edu

[1] P. Neumann, N. Mizuochi, F. Rempp, P. Hemmer, H. Watanabe, S. Yamasaki, V. Jacques, T. Gaebel, F. Jelezko, and J. Wrachtrup, Science **320**, 1326 (2008), ISSN 0036-8075, http://science.sciencemag.org/content/320/5881/1326.full.pdf, URL `http://science.sciencemag.org/content/320/5881/1326`.

[2] M. V. G. Dutt, L. Childress, L. Jiang, E. Togan, J. Maze, F. Jelezko, A. S. Zibrov, P. R. Hemmer, and M. D. Lukin, **316**, 1312 (2007).

[3] W. F. Koehl, B. B. Buckley, F. J. Heremans, G. Caulsine, and D. D. Awschalom, Nature **479**, 84 (2011).

[4] L. C. Bassett, F. J. Heremans, D. J. Christle, C. G. Yale, G. Burkard, B. B. Buckley, and D. D. Awschalom, Science **345**, 1333 (2014).

[5] S.-J. Yu, M.-W. Kang, H.-C. Chang, K.-M. Chen, and Y.-C. Yu, J. Am. Chem. Soc. **127**, 17604 (2005).

[6] A. L. Falk, P. V. Klimov, B. B. Buckley, V. Ivády, I. A. Abrikosov, G. Calusine, W. F. Koehl, A. Gali, and D. D. Awschalom, Phys. Rev. Lett. **112**, 187601 (2014).

[7] V. Jacques, E. Wu, F. Grosshans, F. Treussart, P. Grangier, A. Aspect, and J.-F. Roch, Science **315**, 966 (2007).

[8] J. R. Maze, P. L. Stanwix, J. S. Hodges, S. Hong, J. M. Taylor, P. Cappellaro, L. Jiang, M. V. G. Dutt, E. Togan, A. S. Zibrov, et al., Nature **455**, 644 (2008).

[9] G. Balasubramanian, I. Y. Chan, R. Kolesov, M. Al-Hmoud, J. Tisler, C. Shin, C. Kim, A. Wojcik, P. R. Hemmer, A. Krueger, et al., Nature **455**, 648 (2008).

[10] F. M. Hossain, M. W. Doherty, H. F. Wilson, and L. C. L. Hollenberg, Phys. Rev. Lett. **101**, 226403 (2008).

[11] M. Bockstedte, A. Marini, O. Pankratov, and A. Rubio, Phys. Rev. Lett. **105**, 026401 (2010).

[12] P. Delaney, J. C. Greer, and J. A. Larsson, Nano Lett. **10**, 610 (2010).

[13] J. R. Weber, W. F. Koehl, J. B. Varley, A. Janotti, B. B. Buckley, C. G. Van de Walle, and D. D. Awschalom, Proceedings of the National Academy of Sciences **107**, 8513 (2010),

http://www.pnas.org/content/107/19/8513.full.pdf, URL http://www.pnas.org/content/107/19/8513.abstract.

[14] Y. Tu, Z. Tang, X. G. Zhao, Y. Chen, Z. Q. Zhu, J. H. Chu, and J. C. Fang, Applied Physics Letters **103**, 072103 (2013).

[15] F. Seitz, Rev. Mod. Phys. **18**, 384 (1946).

[16] J. H. Schulman and W. D. Compton, *Color Centers in Solds* (Macmillian, New York, 1962).

[17] J. Lambe and W. D. Compton, Phys. Rev. **106**, 684 (1957).

[18] M.-S. Miao and R. Hoffmann, J. Am. Chem. Soc. **137**, 3631 (2015).

[19] J. H. Schulman and W. D. Compton, *Color Centers in Solds* (Macmillian, New York, 1962).

[20] R. F. W. Bader and J. A. Platts, J. Chem. Phys. **107**, 8545 (1997).

[21] V. V. Rybkin and J. VandeVondele, Journal of Chemical Theory and Computation **12**, 2214 (2016).

[22] F. Illas and G. Pacchioni, The Journal of Chemical Physics **108**, 7835 (1998).

[23] P. Rinke, A. Schleife, E. Kioupakis, A. Janotti, C. Rodl, F. Bechstedt, M. Scheffler, and C. G. Van de Walle, Phys. Rev. Lett. **108** (2012).

[24] F. Karsai, P. Tiwald, R. Laskowski, F. Tran, D. Koller, S. Grafe, J. Burgdorfer, L. Wirtz, and P. Blaha, Phys. Rev. B **89**, 125429 (2014).

[25] P. Tiwald, F. Karsai, R. Laskowski, S. Grafe, P. Blaha, J. Burgdorfer, and L. Wirtz, Phys. Rev. B **92**, 144107 (2015).

[26] B. G. Janesko, J. Chem. Phys. **145**, 054703 (2016).

[27] H. Pick, Z. Phys. **159**, 69 (1960).

[28] A. Meyer and R. F. Wood, Phys. Rev. **133**, A1436 (1964).

[29] A. Szabo and N. S. Ostlund, *Modern quantum chemistry: Introduction to advanced electronic structure theory* (Dover Publications, Inc., Mineola, New York, 1989).

[30] O. V. Gritsenko, P. R. T. Schipper, and E. J. Baerends, J. Chem. Phys. **107**, 5007 (1997).

[31] A. D. Becke, J. Chem. Phys. **112**, 4020 (2000).

[32] D. Cremer, Mol. Phys. **99**, 1899 (2001).

[33] N. C. Handy and A. J. Cohen, Mol. Phys. **99**, 403 (2001).

[34] J. W. Hollet and P. M. W. Gill, J. Chem. Phys. **134**, 114111 (2011).

[35] E. R. Davidson and L. L. Jones, J. Chem. Phys. **37**, 1918 (1962).

[36] E. J. Baerends, Phys. Rev. Lett. **87**, 133004 (2001).

[37] J. S. Bell, Physics, I pp. 195–200 (1964).

[38] C. Kölmel and C. S. Ewig, J. Phys. Chem. B **105**, 8538 (2001).

[39] L. H. Abu-Hassan and P. D. Townes, J. Phys. C: Solid State Phys. **19**, 99 (1986).

[40] O. V. Gritsenko, S. J. A. van Gisbergen, A. Grling, and E. J. Baerends, The Journal of Chemical Physics **113**, 8478 (2000).

[41] K. Burke, J. Chem. Phys. **136**, 150901 (2012).

[42] A. D. Becke, The Journal of Chemical Physics **140**, 18A301 (2014).

[43] H. S. Yu, S. L. Li, and D. G. Truhlar, J. Chem. Phys. **145**, 130901 (2016).

[44] C. D. Sherrill, M. S. Lee, and M. Head-Gordon, Chem. Phys. Lett. **302**, 425 (1999).

[45] L. Noodleman, P. D., and E. J. Baerends, Chem. Phys. **64**, 159 (1982).

[46] K. Yamaguchi, F. Jensen, A. Dorigo, and K. N. Houk, Chemical Physics Letters **149**, 537 (1988).

[47] A. Görling, Phys. Rev. Lett. **85**, 4229 (2000).

[48] S. Grimme and M. Waletzke, The Journal of Chemical Physics **111**, 5645 (1999).

[49] R. Rodriguez-Guzman, K. W. Schmidt, C. Jiménez-Hoyos, and G. E. Scuseria, Phys. Rev. B **85**, 245130 (2012).

[50] T. Tsuchimochi and T. V. Voorhis, The Journal of Chemical Physics **142**, 124103 (2015).

[51] J. P. Perdew, A. Ruzsinszky, L. A. Constantin, J. Sun, and G. I. Csonka, J. Chem. Theory Comput. **5**, 902 (2009).

[52] J. J. Phillips and J. E. Peralta, The Journal of Chemical Physics **135**, 184108 (2011).

[53] E. Runge and E. K. U. Gross, Phys. Rev. Lett. **52**, 997 (1984).

[54] R. Bauernschmitt and R. Ahlrichs, J. Chem. Phys. **104**, 9047 (1996).

[55] M. E. Casida, C. Jamorski, K. C. Casida, and D. R. Salahub, The Journal of Chemical Physics **108**, 4439 (1998).

[56] M. Caricato, G. W. Trucks, M. J. Frisch, and K. B. Wiberg, J. Chem. Theory Comput. **6**, 370 (2010).

[57] N. T. Maitra, J. Chem. Phys. **144**, 220901 (2016).

[58] G. Onida, L. Reining, and A. Rubio, Rev. Mod. Phys. **74**, 601 (2002), URL `https://link.aps.org/doi/10.1103/RevModPhys.74.601`.

[59] E. Rebolini, J. Toulouse, and A. Savin, in *Concepts and Methods in Modern Theoretical Chemistry: Electronic Structure and Reactivity*, edited by S. K. Ghosh and P. K. Chattaraj (CRC

Press, Boca Raton, 2013), pp. 367–389.

[60] J. I. Fuks, A. Rubio, and N. T. Maitra, Phys. Rev. A **83**, 042501 (2011), URL https://link.aps.org/doi/10.1103/PhysRevA.83.042501.

[61] V. Bachler, Journal of Computational Chemistry **30**, 2087 (2009), ISSN 1096-987X, URL http://dx.doi.org/10.1002/jcc.21220.

[62] J. B. Foresman and H. B. Schlegel, in *Recent Experimental and Computational Advances in Molecular Spectroscopy*, edited by R. Fausto (Kluwer Academic Publishers, the Netherlands, 1993), pp. 11–26.

[63] M. Rohrmller, A. Hoffmann, C. Thierfelder, S. Herres-Pawlis, and W. G. Schmidt, Journal of Computational Chemistry **36**, 1672 (2015), ISSN 1096-987X, URL http://dx.doi.org/10.1002/jcc.23983.

[64] R. Kishi and M. Nakano, The Journal of Physical Chemistry A **115**, 3565 (2011).

[65] J. Fan, M. Seth, J. Autschbach, and T. Ziegler, Inorganic Chemistry **47**, 11656 (2008).

[66] Y. Shao, M. Head-Gordon, and A. I. Krylov, J. Chem. Phys. **118**, 4807 (2003).

[67] R. Valero, F. Illas, and D. G. Truhlar, Journal of Chemical Theory and Computation **7**, 3523 (2011).

[68] C. A. Jiménez-Hoyos, T. M. Henderson, T. Tsuchimochi, and G. E. Scuseria, The Journal of Chemical Physics **136**, 164109 (2012).

[69] J. E. Peralta, O. Hod, and G. E. Scuseria, Journal of Chemical Theory and Computation **11**, 3661 (2015).

[70] P. O. Dral and T. Clark, The Journal of Physical Chemistry A **115**, 11303 (2011).

[71] (2014), Gaussian Development Version, Revision I.02+, M. J. Frisch, G. W. Trucks, H. B. Schlegel, G. E. Scuseria, M. A. Robb, J. R. Cheeseman, G. Scalmani, V. Barone, B. Mennucci, G. A. Petersson, H. Nakatsuji, M. Caricato, X. Li, H. P. Hratchian, J. Bloino, B. G. Janesko, A. F. Izmaylov, A. Marenich, F. Lipparini, G. Zheng, J. L. Sonnenberg, W. Liang, M. Hada, M. Ehara, K. Toyota, R. Fukuda, J. Hasegawa, M. Ishida, T. Nakajima, Y. Honda, O. Kitao, H. Nakai, T. Vreven, K. Throssell, J. A. Montgomery, Jr., J. E. Peralta, F. Ogliaro, M. Bearpark, J. J. Heyd, E. Brothers, K. N. Kudin, V. N. Staroverov, T. Keith, R. Kobayashi, J. Normand, K. Raghavachari, A. Rendell, J. C. Burant, S. S. Iyengar, J. Tomasi, M. Cossi, N. Rega, J. M. Millam, M. Klene, J. E. Knox, J. B. Cross, V. Bakken, C. Adamo, J. Jaramillo, R. Gomperts, R. E. Stratmann, O. Yazyev, A. J. Austin, R. Cammi, C. Pomelli, J. W. Ochterski,

R. L. Martin, K. Morokuma, V. G. Zakrzewski, G. A. Voth, P. Salvador, J. J. Dannenberg, S. Dapprich, P. V. Parandekar, N. J. Mayhall, A. D. Daniels, O. Farkas, J. B. Foresman, J. V. Ortiz, J. Cioslowski, and D. J. Fox, Gaussian, Inc., Wallingford CT, 2014.

[72] A. Seidl, A. Görling, P. Vogl, J. A. Majewski, and M. Levy, Phys. Rev. B **53**, 3764 (1996).

[73] A. V. Arbuznikov, M. Kaupp, and H. Bahmann, J. Chem. Phys. **124**, 204102 (2006).

[74] H.-J. Ullrich, A. Uhlig, G. Geise, H. Horn, and H. Waltinger, Mikrochim. Acta **107**, 283 (1992).

[75] W. J. Stevens, H. Basch, and M. Krauss, J. Chem. Phys. **81**, 6026 (1984).

[76] S. H. Vosko, L. Wilk, and M. Nusair, Can. J. Phys. **58**, 1200 (1980).

[77] J. C. Slater, Adv. Quantum Chem. **6**, 1 (1972).

[78] J. P. Perdew, K. Burke, and M. Ernzerhof, Phys. Rev. Lett. **77**, 3865 (1996).

[79] J. P. Perdew, in *Electronic structure of solids '91*, edited by P. Ziesche and H. Eschrig (Akademie Verlag, Berlin, 1991), pp. 11–20.

[80] A. D. Becke, J. Chem. Phys. **107**, 8554 (1997).

[81] P. J. Wilson, T. J. Bradley, and D. J. Tozer, The Journal of Chemical Physics **115**, 9233 (2001).

[82] A. Vásquez-Mayagoitia, C. D. Sherrill, E. Aprà, and B. G. Sumpter, J. Chem. Theory Comput. **6**, 727 (2010).

[83] F. A. Hamprecht, A. J. Cohen, D. J. Tozer, and N. C. Handy, J. Chem. Phys. **109**, 6264 (1998).

[84] A. D. Boese, N. L. Doltsinis, N. C. Handy, and M. Sprik, J. Chem. Phys. **112**, 1670 (2000).

[85] A. D. Boese and N. C. Handy, J. Chem. Phys. **114**, 5497 (2001).

[86] S. Grimme, WIREs Computational Molecular Science **1**, 211 (2011).

[87] J. Tao, J. P. Perdew, V. N. Staroverov, and G. E. Scuseria, Phys. Rev. Lett. **91**, 146401 (2003).

[88] Y. Zhao and D. G. Truhlar, J. Chem. Phys. **125**, 194101 (2006).

[89] J. P. Perdew, M. Ernzerhof, and K. Burke, J. Chem. Phys. **105**, 9982 (1996).

[90] C. Adamo and V. Barone, J. Chem. Phys. **110**, 6158 (1999).

[91] M. Ernzerhof and G. E. Scuseria, J. Chem. Phys. **110**, 5029 (1999).

[92] A. J. Cohen and N. C. Handy, Mol. Phys. **99**, 607 (2001).

[93] A. D. Becke, Phys. Rev. A **38**, 3098 (1988).

[94] A. D. Becke, J. Chem. Phys. **98**, 1372 (1993).

[95] A. D. Becke, J. Chem. Phys. **98**, 5648 (1993).

[96] P. J. Stephens, F. J. Devlin, C. F. Chabalowski, and M. J. Frisch, J. Phys. Chem. **98**, 11623

(1994).

[97] Y. Zhao and D. G. Truhlar, J. Phys. Chem. A **110**, 13126 (2006).

[98] A. Austin, G. A. Petersson, M. J. Frisch, F. J. Dobek, G. Scalmani, and K. Throssell, J. Chem. Theory Comput. **8**, 4989 (2012).

[99] J. Heyd, G. E. Scuseria, and M. Ernzerhof, J. Chem. Phys. **118**, 8207 (2003), **124**, 219906 (2006).

[100] J. Heyd, J. E. Peralta, G. E. Scuseria, and R. L. Martin, J. Chem. Phys. **123**, 174101 (2005).

[101] T. M. Henderson, A. F. Izmaylov, G. E. Scuseria, and A. Savin, J. Chem. Theory Comput. **4**, 1254 (2008).

[102] R. Baer, E. Livshits, and U. Salzner, Annual Review of Physical Chemistry **61**, 85 (2010).

[103] O. A. Vydrov and G. E. Scuseria, J. Chem. Phys. **125**, 234109 (2006).

[104] T. Benighaus, R. A. DiStasio Jr., R. C. Lochan, J.-D. Chai, and M. Head-Gordon, J. Phys. Chem. A **112**, 2702 (2008).

[105] T. Yanai, D. P. Tew, and N. C. Handy, Chem. Phys. Lett. **393**, 51 (2004).

[106] S. Hirata and M. Head-Gordon, Chem. Phys. Lett. **314**, 291 (1999).

[107] A. F. Fix, F. U. Abuova, R. I. Eglitis, E. A. Kotomin, and A. T. Akilbekov, Physica Scripta **86**, 035304 (2012).

[108] A. Ruzsinszky, J. P. Perdew, G. I. Csonka, O. A. Vydrov, and G. E. Scuseria, J. Chem. Phys. **125**, 194112 (2006).

[109] M. Marsman, J. Paier, A. Stroppa, and G. Kresse, J. Phys.: Condens. Mat. **20**, 064201 (2008).

[110] T. M. Henderson, A. F. Izmaylov, G. Scalmani, and G. E. Scuseria, J. Chem. Phys. **131**, 044108 (2009).

[111] K. A. Nguyen, P. N. Day, and R. Pachter, The Journal of Chemical Physics **135**, 074109 (2011).